Complete and incomplete fusion of ^{12}C with ^{165}Ho below 7 MeV/nucleon: Measurements and analysis of excitation functions

Sunita Gupta,[1,*] B. P. Singh,[1] M. M. Musthafa,[2] H. D. Bhardwaj,[3] and R. Prasad[1]
[1]*Department of Physics, Aligarh Muslim University, Aligarh-202002, (U.P.), India*
[2]*Sir Syed College, Thalipparmba, Karimbam, Canannore, (Kerala), India*
[3]*DSN College, Unnao-209801, (U.P.), India*

This experiment has been done with a view to studying complete and incomplete fusion in heavy-ion-induced reactions. Excitation functions for several reactions induced by ^{12}C^{5+} ions on ^{165}Ho at incident energies from 55 to 80 MeV have been measured using the activation technique. The analysis of the data has been done using the codes ALICE-91 and CASCADE. The parameter F_θ, the ratio of actual moment of inertia to the rigid-body value, has been found to play an important role in the calculations done by the code CASCADE. Significant contributions from both the complete and the incomplete fusion channels have been observed. Further, in the case of the reaction $(C,p3n)$ considerable contribution from the decay of higher charge isobar precursor has been observed.

PACS number(s): 25.70.Gh.

I. INTRODUCTION

The study of nuclear reaction mechanism in heavy-ion-(HI) induced reactions has attracted nuclear physicists for many years. Recent literature reports that complete fusion and incomplete fusion are the possible reaction mechanisms in HI-induced reactions [1–4]. At lower excitation energies, the decay of compound nucleus after attaining the thermal equilibrium is the dominant reaction mechanism. However, at moderate excitation energies, preequilibrium (PE) emission also starts competing. The evaporation of the low-energy nucleons may follow PE emission. PE emission reduces the excitation energy of the compound nucleus considerably, leading to an increase in the width of the excitation functions. Further, the number of particles that are subsequently evaporated is reduced.

Depending on the angular momentum carried by the projectile, the process of complete fusion or incomplete fusion of HI's may take place. In the former process, the entire angular momentum of the projectile is transferred to the composite nucleus. However, in the latter one, only a part of the projectile may fuse with the target nucleus and the remaining part is stripped off. This process is also known as breakup fusion. In the process of incomplete fusion, the angular momentum carried by the composite nucleus depends on the mass of the fused fragment [2]. The higher the angular momenta, the smaller the mass of the absorbed fragment. Previous studies of the interaction of ^{12}C with ^{197}Au, and ^{181}Ta by Parket *et al.* [3] and Vergani *et al.* [1,5] provide indications of carbon breakup and fusion of ^{8}Be and α fragments with the target nucleus. Also, the emission of PE nucleons below 10 MeV/nucleon from the composite nucleus created in the complete fusion reaction has been indicated.

As a part of a program to study complete and incomplete fusion in HI-induced reactions, an activation technique has been used to measure the excitation functions for the production of various isotopes in the interaction of ^{12}C with the ^{165}Ho system at incident energies starting below the Coulomb barrier ($\sim$55 MeV) to well beyond it ($\sim$80 MeV). In the present study, theoretical calculations have been done using the computer codes ALICE-91 [6] and CASCADE [7]. The code ALICE-91 performs the compound nucleus calculations along with PE emission, while the code CASCADE performs pure statistical model calculations.

A brief description of the experimental details and formulation is given in Sec. II. Section III is devoted to the experimental uncertainties that are likely to introduce errors in the measured cross sections. Results obtained from the experiment are presented and discussed in Sec. IV. Conclusions drawn from the present studies are given in Sec. V.

II. EXPERIMENTAL DETAILS AND FORMULATION

The experiment has been carried out using the Pelletron accelerator facility at the Nuclear Science Center (NSC), New Delhi, India. Rolled natural Holmium foils (purity $>$99.9%) of thickness $\sim$2 mg/cm^2 were used as target. The α transmission method based on the measurements of the energy lost by α particles while passing through the sample has been utilized to measure the thickness of each target individually. The calibrated ^{241}Am α source was used for these measurements. Individual samples backed by aluminum catcher foils of thickness $\sim$1 mg/cm^2 were irradiated with a ^{12}C^{5+} beam of current $\sim$30 nA at four different energies viz., 55, 62, 71, and 80 MeV. Keeping in view the half-lives of interest, the irradiations were performed for 4–5 h duration each, in the one meter general purpose scattering chamber (GPSC) having invacuum transfer facility. The incident flux of the ^{12}C beam was determined from the charge collected in the Faraday cup using an ORTEC current integrator device, as well as from the counts of the two Rutherford monitors kept at $\pm$30° with respect to the beam direction. They were found to agree with each other within 5%. The activities induced in the target-catcher assembly were

TABLE I. Radioactive properties of residues identified.

Isotope	Half-life	J^π	E_γ (keV)	Abundance(%)
$_{73}\mathrm{Ta}^{174}$	1.18 h	3^+	206.38	57.70
$_{73}\mathrm{Ta}^{173}$	3.65 h	$5/2^-$	172.19	17.00
			180.58	2.10
			701.12	1.20
			1029.90	1.60
$_{73}\mathrm{Ta}^{172}$	36.8 m	3^+	213.96	52.00
			318.75	4.96
			1085.58	7.60
			1109.23	14.00
			1330.33	7.60
$_{72}\mathrm{Hf}^{173}$	23.6 h	$1/2^-$	139.63	12.30
			162.02	6.50
			306.59	6.30
			311.24	10.74
$_{72}\mathrm{Hf}^{171a}$	12.1 h	$7/2^+$	147.11	16.20
			469.20	38.00
			662.25	100.00
			1071.81	56.00
$_{71}\mathrm{Lu}^{171}$	8.24 d	$7/2^+$	739.83	48.10
$_{71}\mathrm{Lu}^{169}$	1.42 d	$7/2^+$	191.21	20.70
$_{71}\mathrm{Lu}^{167}$	51.5 m	$7/2^+$	239.14	8.20
$_{69}\mathrm{Tm}^{167}$	9.24 d	$1/2^+$	207.79	41.00
$_{69}\mathrm{Tm}^{165}$	1.25 d	$1/2^+$	218.79	2.40

[a]Relative abundance of characteristic γ lines.

followed off line, using a high-resolution (2 keV for 1.33 MeV γ ray of ^{60}Co) HPGe detector of 100 cm^3 active volume coupled to the ORTEC's PC-based multichannel analyzer. The HPGe spectrometer was calibrated using various standard sources, i.e., ^{22}Na, ^{54}Mn, ^{57}Co, ^{60}Co, ^{133}Ba, ^{137}Cs, and ^{152}Eu of known strengths. The γ-ray spectra recorded at increasing times were analyzed employing the ORTEC's peak fitting program MCA. The residues were identified by their characteristic γ radiations and half-lives. The intensities of these γ rays have been used to compute the experimental cross sections corresponding to the various radioactive residues. The half-lives of the residual nuclei, characteristic γ-ray energies, abundance, etc., are taken from the Table of Isotopes [8] and are given in Table I. The geometry-dependent efficiency ($G\varepsilon$) of the detector for different source-detector distances was computed using the relation

$$G\varepsilon = N_0 / N_{a0} e^{-\lambda t} \theta, \qquad (1)$$

where N_0 is the disintegration rate at the time of measurement, N_{a0} is the disintegration rate at the time of manufacture, λ is the decay constant, t is the time lapse between the manufacture of the source and the start of counting, θ is the branching ratio of the γ ray. The standard γ sources were used for this purpose. The values of $G\varepsilon$ thus obtained, were plotted as a function of energy using the program GRAPHER.

TABLE II. Measured cross sections for the production of Ta isotopes.

E_{lab} (MeV)	$\sigma(^{174}\mathrm{Ta})$ (mb)	$\sigma(^{173}\mathrm{Ta})$ (mb)	$\sigma(^{172}\mathrm{Ta})$ (mb)
55.0 ± 1.1	46 ± 6	13 ± 2	
62.0 ± 0.9	62 ± 8	200 ± 27	
71.0 ± 1.0	11 ± 2	336 ± 44	83 ± 11
80.0 ± 0.9	2 ± 0.3	122 ± 16	287 ± 38

A polynomial of degree 5 having the following form was found to give the best fit for these curves:

$$G\varepsilon = a_0 + a_1 X + a_2 X^2 + a_3 X^3 + a_4 X^4 + a_5 X^5 \qquad (2)$$

with coefficients a_0, a_1, a_2, a_3, a_4, a_5 having different values for different source-detector distances, X being the energy of the characteristic γ ray.

In the case of mixing of γ rays originated from different isotopes, the contribution from each isotope has been separated on the basis of their half-lives, by following the induced activity for a considerably long period. Further, the same residual nucleus may be produced by the activation and by the decay of higher charge isobar precursor nucleus through β emission or electron capture (EC). In such cases, the characteristic γ-ray intensity has contributions from both the channels. In the case presently studied, the half-life of the precursor is considerably smaller than that of the residue. Therefore, the cumulative cross sections have been determined by analyzing the induced activities at times greater than about eight to ten half-lives of the precursor. The cumulative cross section of a given residue is the sum of (i) its independent production cross section (ii) cross section for the independent production of its precursor multiplied by a numerical coefficient which depends on the branching ratio for precursor decay to residue, and the half-lives of the precursor and the residue. The following decay analysis given by Cavinato et al. [9] has been used in order to obtain the precursor decay contributions.

If a precursor P is formed with cross section σ_P during the irradiation, and decays with half-life $T_{1/2}^P$ and a branching ratio P_P, to a daughter nucleus D which is produced with cross section σ_D during the irradiation and decays with half-life $T_{1/2}^D$, the cumulative cross section σ_C for the production of daughter is given by

$$\sigma_C = \sigma_D + P_P [T_{1/2}^D / (T_{1/2}^D - T_{1/2}^P)] \sigma_P. \qquad (3)$$

TABLE III. Measured cross sections for the production of Hf isotopes.

E_{lab} (MeV)	$\sigma(^{173}\mathrm{Hf})$ (mb)		$\sigma(^{171}\mathrm{Hf})$ (mb)
	Cumulative	Independent	Cumulative
62.0 ± 0.9	248 ± 33	11 ± 2	
71.0 ± 1.0	843 ± 112	446 ± 60	
80.0 ± 0.9	547 ± 73	404 ± 54	145 ± 22

In the case of the residual nucleus emitting γ rays of more than one energy, the cross section for the same reaction has been determined separately from the observed intensities of all the identified γ rays. The weighted cross section [10] is taken as the final experimental value.

The experimentally measured reaction cross sections σ_r, are computed using the following expression [11]:

$$\sigma_r = A\lambda \exp(\lambda t_2)/N_0 \phi \theta K(G\varepsilon)$$
$$\times \{1 - \exp(-\lambda t_1)\}\{1 - \exp(-\lambda t_3)\}, \qquad (4)$$

where A is the observed counting rate, N_0 is the number of target nuclei, ϕ is the incident beam flux, t_1 is the time of irradiation, λ is the decay constant of the residual nucleus, t_2 is the time lapse between the stop of irradiation and start of counting, t_3 is the data accumulation time, θ is the branching ratio of the characteristic γ ray, $G\varepsilon$ is the geometry-dependent efficiency of the detector, K is the self-absorption correction term.

III. EXPERIMENTAL UNCERTAINTIES IN THE MEASUREMENTS

Apart from the errors due to the uncertainty of the nuclear data, like the branching ratio, decay constants, etc., the inaccurate estimate of the foil thickness may lead to an uncertainty in determining the number of target nuclei and may introduce errors in the measured cross sections. The error in the thickness of the sample material is expected to be <1%. Errors may arise due to fluctuation in beam current. These were minimized by continuously monitoring it. An accidental stop of beam (if any) and any appreciable fluctuation of the beam intensity during the irradiation was taken care of while calculating the total irradiation time. It is estimated that in the present experiment, the beam current fluctuations may introduce <3% errors. Uncertainty in the fitting of the efficiency curve (<3%) and also the solid angle effect (<2%) [12] may lead to inaccuracy in the measurement of detector efficiency. The statistical error in the counting of the standard source was minimized by accumulating data for a comparatively longer time (~3000 s). The statistical fluctuation in efficiency is estimated to be <2%. In order to minimize the loss due to the nuclei recoiling out of the target, the sample and the catcher foil were counted together. Error in the incident beam energy has been determined by calculating the energy spread in half of the sample thickness with the help of the stopping power tables of Northcliffe and Schilling [13]. In addition, there may be an inherent energy uncertainty in the beam energy.

IV. EXPERIMENTAL RESULTS AND DISCUSSION

A. Results

Reaction cross sections at different incident energies starting near the Coulomb barrier to well above it have been measured for the reactions

TABLE IV. Measured cross sections for the production of Lu isotopes.

E_{lab} (MeV)	$\sigma(^{171}$Lu) (mb)	$\sigma(^{169}$Lu) (mb)	$\sigma(^{167}$Lu) (mb)
62.0±0.9	11±2	14±2	6±1
71.0±1.0	19±3	19±3	7±1
80.0±0.9	140±21	21±3	36±5

^{165}Ho(C,3n)^{174}Ta, ^{165}Ho(C,4n)^{173}Ta, ^{165}Ho(C,5n)^{172}Ta,

^{165}Ho(C,p3n)^{173}Hf, ^{165}Ho(C,p5n)^{171}Hf, ^{165}Ho(C,α2n)^{171}Lu,

^{165}Ho(C,α4n)^{169}Lu, ^{165}Ho(C,α6n)^{167}Lu,

^{165}Ho(C,2α2n)^{167}Tm, ^{165}Ho(C,2α4n)^{165}Tm.

A brief description of how these isotopes may be formed through different reaction channels is given here. These isotopes can be formed by the complete fusion of ^{12}C with ^{165}Ho followed by the emission of the n, p, and/or α particle. In addition to this, Hf isotopes may also be produced in the decay of the higher charge precursor Ta isobars. In the case of ^{173}Hf, the cumulative cross section has been determined by following the activities at times longer than about 8–10 half-lives of the precursor because of the comparatively shorter half-life of the precursor [represented by filled triangles in Fig. 2(a)]. The independent cross section for the production of ^{173}Hf has been determined using the following expression:

$$\sigma_{cum} = \sigma(^{173}Hf) + 1.18296\sigma(^{173}Ta) \qquad (5)$$

obtained from Eq. (3) and are shown by filled circles in Fig. 2(a). In the case of ^{171}Hf, only the cumulative cross section for its production has been obtained, because the cross section for the production of its precursor, i.e., ^{171}Ta could not be computed due to its complex mixing with γ rays from other channels. Similarly, the Lu isotopes may also be formed in the decay of the higher charge isobar precursors of Ta and Hf. Another channel for the production of these isotopes may be the incomplete fusion of ^{8}Be fragment (if ^{12}C undergoes breakup into α and ^{8}Be fragments) followed by the emission of neutrons. The contribution of ^{171}Lu isotope from the precursor decay of ^{171}Hf at 62 and 71 MeV is expected to be negligible because of the relatively high value of threshold energy (~62 MeV) for the latter. However, at 80 MeV, the measured cross section for ^{171}Lu is cumulative. Moreover, the Tm isotopes may be formed by the incomplete

TABLE V. Measured cross sections for the production of Tm isotopes.

E_{lab} (MeV)	$\sigma(^{167}$Tm) (mb)	$\sigma(^{165}$Tm) (mb)
62.0±0.9	5±1	99±14
71.0±1.0	34±4	336±47
80.0±0.9	109±15	252±37
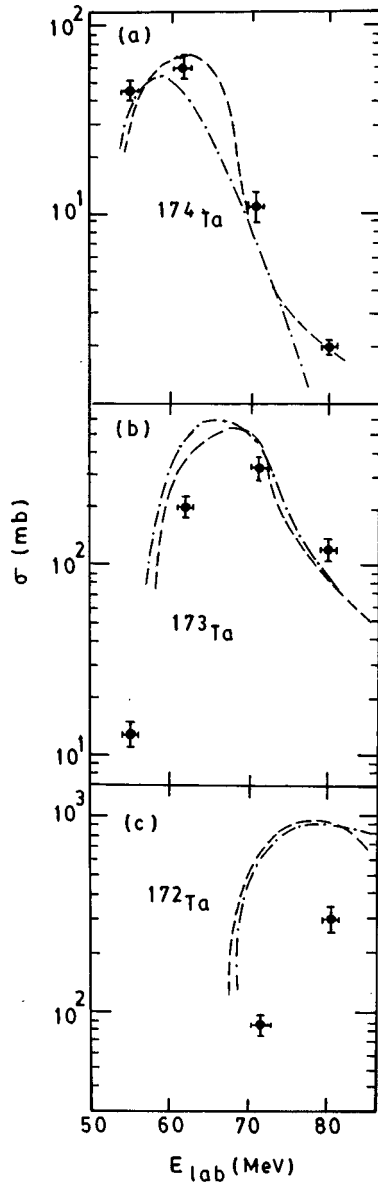
FIG. 1. Excitation functions for ^{165}Ho(C,$3n$)^{174}Ta, ^{165}Ho(C,$4n$)^{173}Ta, and ^{165}Ho(C,$5n$)^{172}Ta reactions. The filled circles represent the experimental data. The dashed curve corresponds to the theoretical predictions of the code ALICE-91 with n_0 = 12. The compound nucleus calculations are represented by the dash-dotted curve.

fusion of α fragment (if ^{12}C undergoes breakup into α and ^{8}Be fragments). The presently measured cross sections for the production of Ta, Hf, Lu, and Tm isotopes at different incident energies are given in Tables II, III, IV, and V, respectively, and are shown graphically in Figs. 1–7.

B. Discussion

1. Analysis with code ALICE-91

The code ALICE-91 facilitates the calculations for both equilibrium and PE emission cross sections. In this code the Weisskopf-Ewing model [14] is employed for compound
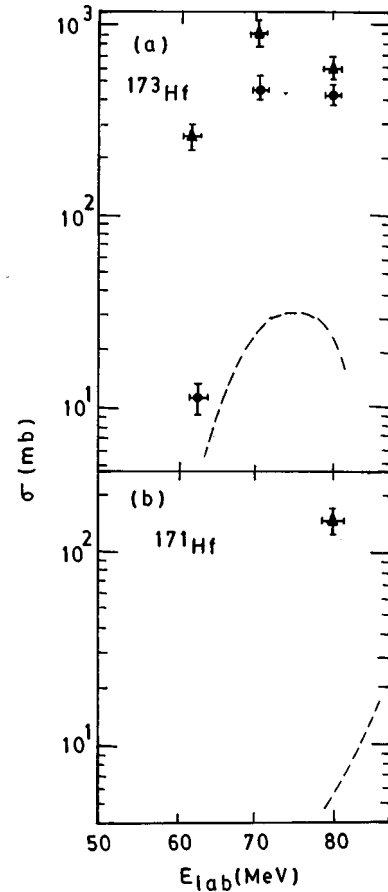
FIG. 2. Excitation functions for the ^{165}Ho(C,$p3n$)^{173}Hf and ^{165}Ho(C,$p5n$)^{171}Hf reactions. The experimental data including the precursor contribution is indicated by filled triangles. In (a) the filled circles represent the cross section for the independent production of the ^{173}Hf isotope obtained by the procedure described in the text. The dashed curve corresponds to the theoretical predictions of the code ALICE-91 with n_0 = 12.

nucleus calculations and the PE component is simulated using the Hybrid model [15]. Further, it does not take into account the possibility of incomplete fusion. Like all semi-classical models, in ALICE-91 calculations the equipartition of energy among the initial excited particles and holes is assumed, which in the case of HI reactions may not be a very good approximation. In general, the input parameters, initial exciton number n_0 and the mean free path multiplier COST largely govern the PE contribution, while the level density parameter a affects the equilibrium component. The level density parameter constant K has been calculated from the expression $a=A/K$, where, A is the atomic mass of the compound system. The value of a for the system has been taken from Dilg tables [16] for the back-shifted Fermi-gas model. In the present calculations, the experimental data is satisfactorily reproduced with $K=9.5$. For the separation energies and level density ground-state shifts, we have used the option that substitutes Gove mass tables [17] for Myers-Swiatecki-Lysekil masses [18] including shell corrections. Inverse cross sections have been calculated by optical model subroutine and the parameters of Becchetti and Greenlees have been used. The initial exciton configuration n_0 = 12
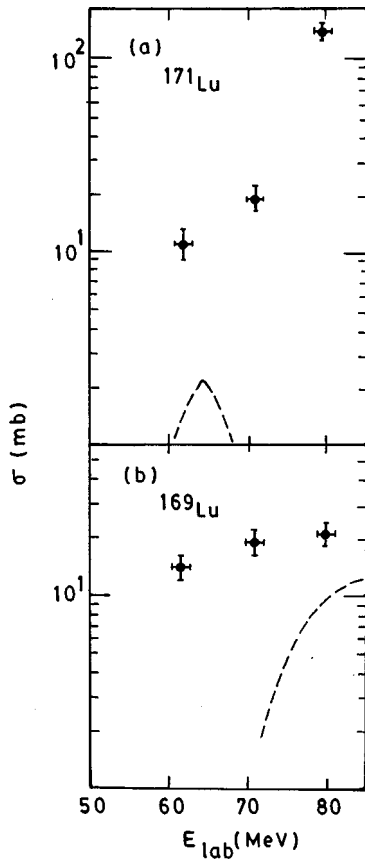
FIG. 3. Excitation functions for the ^{165}Ho(C,$\alpha 2n$)^{171}Lu and ^{165}Ho(C,$\alpha 4n$)^{169}Lu reactions. The filled circles represent the experimental data. The dashed curve corresponds to the theoretical predictions of the code ALICE-91 with $n_0 = 12$.

($n_n = 6$, $n_p = 6$, $n_h = 0$), which is equivalent to the breakup of incident ^{12}C ion in the field of the nucleus and the nucleons occupying excited states above the Fermi energy has been taken in the present calculations. The calculations done assuming $n_0 = 12$ satisfactorily reproduces the measured excitation functions for (C,xn) ($x = 3,4$) reactions at higher energies. Further, the peaks of the measured excitation functions were observed to be shifted towards the higher energy side in comparison to the corresponding calculations with the code ALICE-91. This may be attributed to the fact that in HI reactions the projectile imparts large angular momentum to the composite system. If, in the last stages of nuclear deexcitation, higher angular momentum inhibits particle emission more than it does γ emission, then, the peak of the excitation function corresponding to the particle emission mode will be shifted to higher energy [19]. A similar shift may also be produced if the mean energy of the evaporated particles increases with increasing nuclear spin. One may obtain an estimate of the possible size of an overall energy shift from the nuclear rotational energy. For a rigid-body moment of inertia $E_{rot} \sim (m/M)E_{lab}$, where m/M is the ratio of the projectile and target masses and E_{lab} is the incident energy [19]. In the present case at incident energies 55, 62, 71, and 80 MeV the rotational energy varies from 4 to 5.8 MeV. The effect is more pronounced in HI reactions as com-
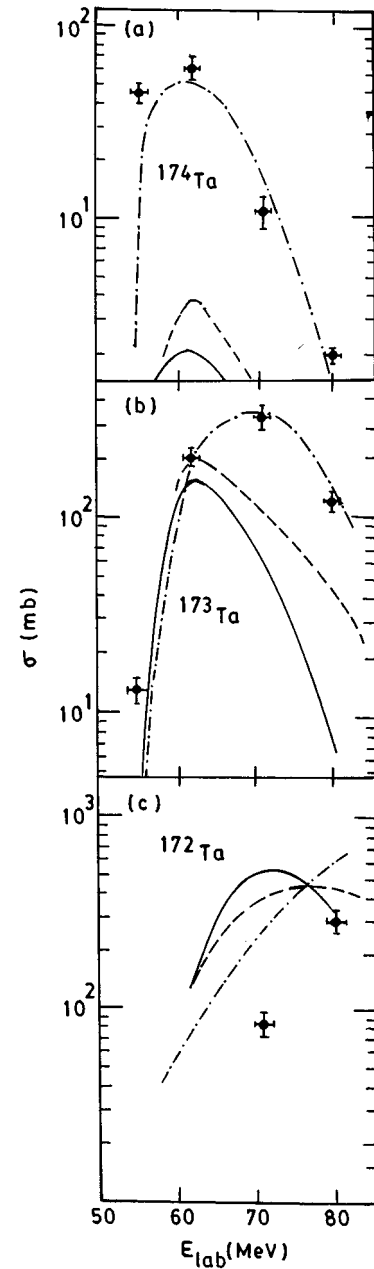

FIG. 4. Excitation functions for the ^{165}Ho(C,3n)^{174}Ta, ^{165}Ho(C,4n)^{173}Ta, and ^{165}Ho(C,5n)^{172}Ta reactions. The filled circles represent the experimental data. The theoretical predictions of the code CASCADE with $F_\theta = 0.15$, $F_\theta = 0.50$, and $F_\theta = 0.85$ (default value) are represented by dash-dotted, dashed, and solid curves, respectively.

pared to the light ion reactions, since the rotational energy is much greater in case of HI reactions. Since the angular momentum effects have not been considered in the pure Weisskopf-Ewing calculations of the present version of the code, it is desirable to shift the calculated excitation functions by the amount approximately equal to E_{rot} as calculated above. It has been observed that the ALICE-91 calculations satisfactorily reproduce the experimental data when the energy scale of the calculated excitation functions are shifted
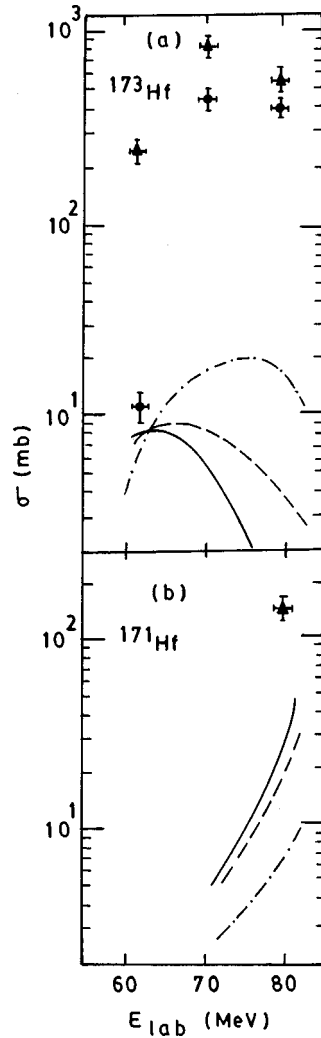
FIG. 5. Excitation functions for the ^{165}Ho(C,$p3n$)^{173}Hf and ^{165}Ho(C,$p5n$)^{171}Hf reactions. The figure caption is the same as that for Fig. 2 with the theoretical predictions of the code CASCADE with $F_\theta=0.15$, $F_\theta=0.50$, and $F_\theta=0.85$ (default value) represented by dash-dotted, dashed, and solid curves, respectively.

by respective $E_{\rm rot}$ values. The experimentally measured and theoretically calculated excitation functions are shown in Figs. 1(a)–1(c), for (C,xn) ($x=3-5$) reactions. Surprisingly, the ALICE-91 calculations for (C,5n) do not match with the experimental results but the overall shape of the excitation function is reproduced.

2. Analysis with code CASCADE

The statistical code CASCADE [7] is based on Hauser-Feshbach theory [20]. It does not take into account the possibility of fission, PE emission, and/or incomplete fusion. A formula derived from the Fermi-gas model is used for calculating the level densities for the product nuclei. The general input data, like the mass of nuclides and the transmission coefficients for the emitted particles have been computed using the computer codes MASS and TLCALC, respectively, for the range of interest and stored permanently on the disc. The transmission coefficients in these calculations were generated
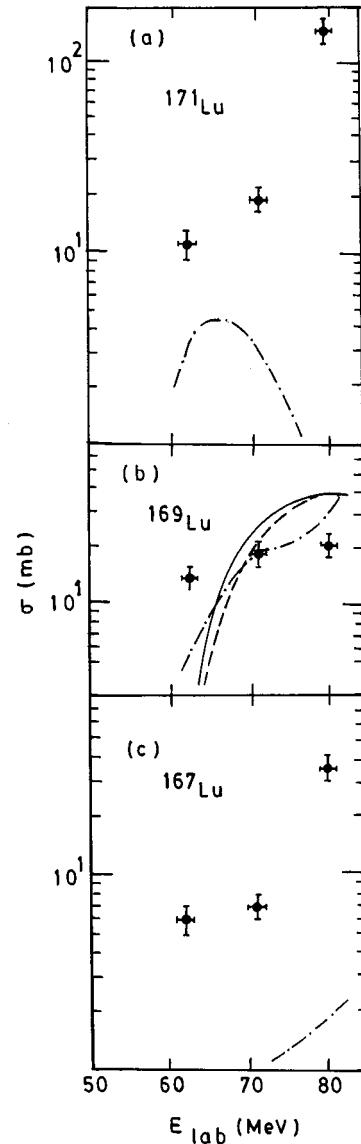

FIG. 6. Excitation functions for the ^{165}Ho(C,$\alpha2n$)^{171}Lu, ^{165}Ho(C,$\alpha4n$)^{169}Lu, and ^{165}Ho(C,$\alpha6n$)^{167}Lu reactions. The filled circles represent the experimental data. The theoretical predictions of the code CASCADE with $F_\theta=0.15$, $F_\theta=0.50$, and $F_\theta=0.85$ (default value) are represented by dash-dotted, dashed, and solid curves, respectively.

using the optical model potentials of Becchetti and Greenlees [21] for neutrons and protons and that of Satchler [22] for α particles. The value of the level density parameter constant K chosen here is the same as the one used in the code ALICE-91. As may be observed from Figs. 4(a)–4(c), the measured excitation functions are not consistently reproduced by the calculations done with the default set of parameters. In an attempt to consistently reproduce the measured excitation functions using this code, the sensitiveness of calculations to the values of input parameters has been studied. In particular, the parameter F_θ, which is the ratio of the actual moment of inertia to the rigid-body moment of inertia of the excited system, has been found to affect the calculated excitation functions considerably. The default value of $F_\theta(=0.85)$ does
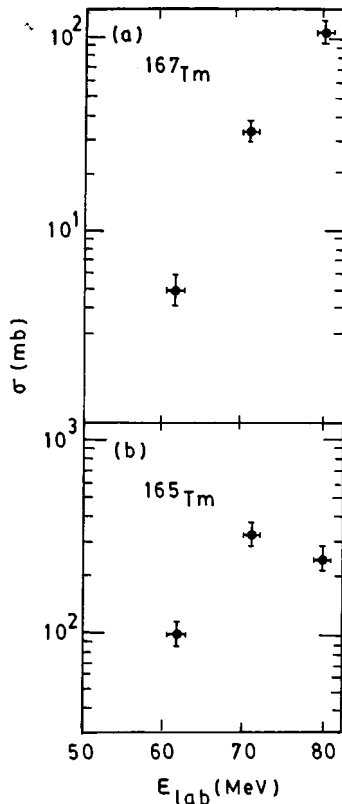
FIG. 7. Experimentally measured excitation functions for the ^{165}Ho(C,$2\alpha2n$)^{167}Tm and ^{165}Ho(C,$2\alpha4n$)^{165}Tm reactions.

not reproduce the measured excitation functions. Moreover, a value of F_θ equal to 0.50 obtained from the rotational energy bands of the ^{177}Ta nucleus [23] also does not reproduce the measured excitation functions. However, a value of F_θ equal to 0.15 gives satisfactory reproduction of the measured excitation functions. It may be pointed out that this anomalous value of the parameter F_θ is unlikely in such reactions.

It may be noticed from Figs. 2 and 5 that both these codes do not satisfactorily reproduce the experimental data for (C,$p3n$) and (C,$p5n$) reactions. Figures 3 and 6 also indicate that the experimental results for (C,αxn) ($x=2,4,6$) channels do not match with the theoretical predictions. Further, the experimentally measured cross sections for the pro-

duction of ^{167}Tm and ^{165}Tm isotopes via (C,$2\alpha xn$) ($x=2,4$) reaction channels, respectively, are shown in Figs. 7(a) and 7(b). Both the codes ALICE and CASCADE predict negligible cross sections for these reaction channels and, as such, corresponding theoretical calculations are not shown in these figures. The enhancement in the experimental cross sections for (C,αxn) and (C,$2\alpha xn$) channels as compared to theoretical predictions may be attributed to the fact that these channels are populated not only by the complete fusion of ^{12}C with ^{165}Ho but also through the incomplete fusion of ^{8}Be and ^{4}He with ^{165}Ho, respectively.

V. CONCLUSIONS

The excitation functions for ten reactions induced by ^{12}C incident on ^{165}Ho have been measured employing activation technique. In the analysis with code ALICE-91, there are indications of some PE emission. A value of $n_0=12$ is found to satisfactorily reproduce the measured excitation functions for the complete fusion channels. In the calculations with code CASCADE, which does not include PE emission, the default set of parameters do not reproduce the measured excitation functions and the role of the parameter required for scaling the moment of inertia is found to be quite important. Further, the theoretical calculations suggest that at higher incident energies, the Lu isotopes formed via (C,αxn) reactions may be produced by the evaporation of one α particle and neutrons. However, the enhancement in the experimentally measured cross sections for Lu and Tm isotopes at incident energies 62, 71, and 80 MeV, as opposed to the theoretical predictions, indicate that the major contribution to their production may come from the incomplete fusion of ^{8}Be and α fragments. This is also supported by the α cluster structure of ^{12}C.

[1] P. Vergani, E. Gadioli, E. Vaciago, E. Fabrici, E. Gadioli Erba, M. Galmarini, G. Ciavola, and C. Marchetta, Phys. Rev. C **48**, 1815 (1993).

[2] M. Crippa, E. Gadioli, P. Vergani, G. Ciavola, C. Marchetta, and M. Bonardi, Z. Phys. A **350**, 121 (1994).

[3] D. J. Parker, P. Vergani, E. Gadioli, J. J. Hogan, F. Vettore, E. Gadioli Erba, E. Fabrici, and M. Galmarini, Phys. Rev. C **44**, 1528 (1991).

[4] B. B. Kumar, S. Mukherjee, S. Chakrabarty, B. S. Tomar, A. Goswami, and S. B. Manohar, Phys. Rev. C **57**, 743 (1998).

[5] P. Vergani, E. Gadioli, E. Vaciago, E. Guazzoni, L. Zetta, G.

Ciavola, M. Jaskola, P. L. Dellera, V. Campagna, and C. Marchetta, Report No. INFN/BE 92/02 (unpublished).

[6] M. Blann, NEA Data Bank, Gif-sur-Yvette, France, Report No. PSR-146, (1991).

[7] F. Puhlhofer, Nucl. Phys. **A280**, 267 (1977).

[8] E. Browne and R. B. Firestone, *Table of Radioactive Isotopes* (Wiley, New York, 1986).

[9] M. Cavinato, E. Fabrici, E. Gadioli, E. Gadioli Erba, P. Vergani, M. Crippa, G. Colombo, I. Redaelli, and M. Ripamonti, Phys. Rev. C **52**, 2577 (1995).

[10] S. F. Mughabghab, M. Divadeenam, and N. E. Holden, *Neu-*

tron Cross-sections 1A (Academic, New York, 1981), p. 89.

[11] B. P. Singh, M. G. V. Sankaracharyulu, M. Afzal Ansari, R. Prasad, and H. D. Bhardwaj, Phys. Rev. C **47**, 2055 (1993).

[12] R. P. Gardner and K. Verghese, Nucl. Instrum. Methods **93**, 163 (1971).

[13] L. C. Northcliffe and R. F. Schilling, At. Data Nucl. Data Tables A **7**, 264 (1970).

[14] V. F. Weisskopf and D. H. Ewing, Phys. Rev. **57**, 472 (1940).

[15] M. Blann, Phys. Rev. Lett. **27**, 337 (1971).

[16] W. Dilg, W. Schantl, H. Vonach, and M. Uhl, Nucl. Phys. **A217**, 269 (1973).

[17] N. B. Gove and A. H. Wapstra, Nucl. Data Sheets **9**, 242 (1971).

[18] W. D. Myers and W. J. Swiatecki, Nucl. Phys. **B1**, 1 (1966).

[19] D. Bodansky, Annu. Rev. Nucl. Sci. **12**, 79 (1962).

[20] W. Hauser and H. Feshbach, Phys. Rev. **87**, 336 (1952).

[21] F. D. Becchetti and G. W. Greenlees, Phys. Rev. **182**, 1190 (1969).

[22] G. R. Satchler, Nucl. Phys. **70**, 177 (1965).

[23] Y. A. Ellis and B. Harmatz, Nucl. Data Sheets **16**, 154 (1975).